CHAPTER-2
Thin Film Growth and Characterization Techniques

2.1 Thin Films Growth Techniques

The fabrication of thin films is the first step towards the development of electronic devices. When hybrid hetero-structures must integrate, thin films become highly significant, and it is possible to fabricate stable, good adhesion and homogeneous thin films to explore the characteristics of II-VI compound semiconductor materials. Thin-film materials are essential components of today's technical developments in optoelectronic, photonic, and magnetic devices. The detailed analysis of thin-film features such as structural, optical, and electrical properties has become an important aspect of technological device research and development. As the thin film properties are extremely sensitive to the deposition techniques, several growth techniques have been developed (depends on the desired film properties) for the deposition of various types of thin films on a wide range of substrates, including polymers, alloys, metals, ceramics, and superconductors. Each deposition process has advantages and disadvantages. No one technique can deposit thin films that account for all of the desired factors, such as deposition circumstances, equipment costs, and substrate type.

Flexible thin-film materials have different qualities that are usually distinct from those of bulk materials due to their physical and chemical properties. The thin films (II-VI compound semiconductors) are grown by various evaporation physical and chemical techniques such as chemical bath deposition [55], atomic layer deposition [64], molecular beam epitaxy [60], sputtering [54, 127], thermal evaporation [52, 53], pulsed laser deposition [57, 128], spray pyrolysis [58, 59], sol-gel [61], metal-organic chemical vapor deposition [63], close-spaced sublimation [62] and successive ionic layer adsorption and reaction method (SILAR) [65]. In this present dissertation work, the evaporation and

sputtering growth techniques have been used to deposit CdS, CdTe, Mo-Ni, and Molybdenum oxides thin films. The basic steps of thin films deposition are-

(1) Using appropriate procedures to produce atomic or molecular materials.

(2) Material condensation n on the substrate, followed by nucleation and development of a thin film.

(3) Using a medium to transport these components to the substrate.

Thin-film deposition techniques are divided into two categories [129].

a.) Physical techniques

b.) Chemical techniques

Physical methods cover deposition techniques (e.g., evaporation techniques or sputtering mechanism) that rely on the ejection or evaporation of material from a source material, whereas chemical technique rely on specific chemical mechanism or interaction, which in anodization and electroplating may rely on the electrical separation of ions [130]. To obtain thin films in all of these circumstances, however, a specific chemical reaction is required. Chemical methods for film growth can be divided into two categories: the first is concerned with the chemical production of the film from medium, while the second is concerned with the development of thin-film from precursor materials such as thermal growth, iodization, and gaseous iodization.

Table 2.1 summarises the many physical and chemical processes that are commonly employed to deposit thin films. Pulsed laser deposition, atomic layer, and molecular layer depositions, all of these are advanced deposition techniques, can also be used to deposit thin films. Physical vapor deposition method have received increased attention since they

allow for control of stoichiometry, porosity, film growth rate, and film microstructure, all of which may be adjusted by changing the deposition circumstances.

Table 2.1: Thin-film growth processes classified by physical and chemical techniques. (http://shodhganga.inflibnet.ac.in/bitstream/10603/4023/8/08_chapter%202)

Thin Film Deposition Techniques			
Physical Methods		**Chemical Methods**	
Evaporation	**Sputtering**	**Liquid Phase**	**Gas Phase**
Flash	Getter Sputtering	Chemical Bath Deposition	Laser Chemical Vapor Deposition
Vacuum	Glow Discharge DC	Electro-deposition	Chemical Vapor Deposition
Electron Beam	Ion Beam Sputtering	Atomic & Molecular Beam Epitaxy	Metal-Organo Chemical Vapour Deposition
Thermal	R.F. Magnetron Sputtering	Electro-less deposition	Plasma Enhanced Deposition
Laser	High target utilization	Sol-gel	
R.F. Heating	Reactive	Anodisation	
Arc Heating		Spin-coating	
Resistive Heating	Pulsed DC sputtering	Polymer Assisted Deposition	
		Spary-pyrolysis	
		Screen Printing	
		Ultrasonic	

Evaporation (thermal and e-beam) and sputtering procedures are the most adaptable of these techniques for growing thin films of a wide range of materials. Out of these strategies, RF sputtering method was employed in this thesis work.

2.1.1 Vacuum Evaporation

This method is so simple and convenient, it is the most extensively used technology for preparing thin films for the deposition of materials, alloys, metals, and other substances. The basic requirement is a vacuum atmosphere in which sufficient heat is applied to the evaporating materials to provide the required vapor pressure for evaporation. The evaporated substance is allowed to deposit on a temperature-controlled substrate. To dissipate the charge, a resistively heated tantalum or tungsten source is employed. The evaporation rate, the temperature of the substrate, oxygen partial pressure, and source-to-substrate distance are all crucial control parameters. Evaporation of transparent conductors can be accomplished in three ways:

i.) Metal oxides evaporate directly,

ii.) Reactive evaporation of the metal in the presence of oxygen, and

iii.) When an oxide substance is evaporated, there will always be some oxygen deficiency. To avoid this, the films must be deposited in partial oxygen pressure or undergo some post-deposition heat mechanism in the air.

Reactive evaporation of either an oxide or a metallic alloy combination is used in reports on the formation of ITO thin films via evaporation [131-134]. Films formed by vacuum evaporation employing oxide mixtures are often oxygen deficiencies, and transparent thin films require an oxygen partial pressure of 10^{-4} Torr. Even for highly doped films, the X-ray diffraction method of vacuum evaporated ITO films found no trace of any tin oxide phase [135]. In vacuum evaporated films, the optimum orientation was observed to be (111). In this investigation, the metal electrodes were deposited using the thermal evaporation process.

2.1.2 Pulsed laser deposition

Pulsed laser deposition (PLD) is a unique method for producing superconducting and transparent conducting thin films. In the formation of multicomponent oxide thin films, PLD has significant benefits over conventional deposition processes. [136] For a multi-component target, the PLD-grown films have the same composition as the target. Due to the high kinetic energy (K.E) i.e.>1 eV of the ejected and ionized specimen in the laser-generated plasma, PLD films crystallize at a lower substrate temperature than other physical vapor deposition processes. The TCO film generated using PLD also has an extremely flat surface. PLD-grown ITO films have been employed as the anode contact in organic light-emitting diodes. The low deposition rates, small substrate coverage, and non-uniformity of the thickness of thin films are the key challenges facing PLD technology.

2.1.3 Chemical vapor deposition

One of the most common ways for generating semi-conductive transparent thin films is chemical vapor deposition (CVD). A reaction of one or more gaseous reactive species on a solid substrate is used in this technique. Metallic oxides are formed by vaporizing an appropriate organometallic chemical. A vapor containing the condensate material is transferred to a substrate surface, where it undergoes a heterogeneous decomposition process [137]. To avoid the production of powdery deposits, which can cause haziness in the films, the decomposition condition should be such that the reaction happens only at or near the substrate surface and not in the gaseous phase.

The quality of CVD-deposited films is determined by many factors, including system geometry, substrate temperature, and gas flow rate. To get the greatest quality films, all of these characteristics should be tuned and regulated. The important features of utilizing the

CVD method are its ease, simplicity, and reproducibility with which it may be used for large-scale manufacturing without the need for vacuum. The cost of producing thin films using this method is quite low. It is possible to produce thin films with structural perfection, stoichiometry, and excellent purity. The main disadvantage is that the type of the chemical change and the activation process substantially influence the morphology of the films produced by CVD.

2.1.4 Thermal Evaporation

Evaporation methods are commonly employed for the preparation of thin films. When evaporation takes place in a vacuum, the evaporation temperature drops dramatically, reducing the number of contaminants in the developing layer. To evaporate a substance in a vacuum, a vapor source is necessary, which delivers both heat and the charge of evaporator needed to reach a high temperature and produce the desired vapor pressure. The supporting material must have a minimal vapor pressure and dissociation temperature of the working temperature to minimize contaminants in the evaporant and growing film. [138] The most extensively used process for preparing thin films is thermal evaporation, in which the material is heated in a vacuum chamber under a high vacuum until fusion occurs by running an electrical current through a filament or metal plate where the material is deposited. After that, the evaporated substance condenses on the substrate. [139] It is an excellent idea to fabricate high-quality thin films of any thickness on a variety of flexible substrates, including plastic, glass, and metals. Within the vacuum coating chamber, resistive heating is utilized to vaporize the required substance, which then adheres to the substrate.

The transmittance, reflectance, and absorption of light can be precisely regulated by depositing thin layers of source material on the substrates. The coating chamber of batch coaters must be opened during each deposition procedure whenever the substrate or evaporation material is replaced, whereas serial coaters are meant to operate continuously. As a result, a computer-controlled system automatically refills the substrate and evaporation material after one process. The substrate holder is located inside the coating chamber, and each substrate is placed on the holder over a rotating crucible or boat. The chamber is kept at a high vacuum after the substrate is deposited on the holder to ensure that the atoms of the evaporated substance may attach to the substrate. The mean free path between successive impacts becomes large only at high pressure (10^{-5} torr), allowing the vapor beam to arrive at the substrate without scattering and the evaporant to proceed straight and condense on the substrate. When a low vacuum is utilized, gas molecules collide with the substrate, contaminating the deposited films. [140] Crucibles constructed of inert materials with excellent heat tolerance, such as oxygen-free copper, tantalum, tungsten, and molybdenum, are commonly employed in this technique. To reduce the chances of reactions, the crucibles are usually covered with alumina. The thermal evaporation approach offers several advantages, including a high deposition rate, reduced material consumption, and a cost-effective deposition procedure.

2.1.5 E-beam Evaporation

This is a similar technique to thermal evaporation, in which source material is heated above its sublimation temperature and evaporated to produce a layer on the substrate's surfaces. Instead of resistive heating in vacuum coating, this approach uses electron bombardment to increase the temperature of the source materials. Using a thermionic generating tungsten

metal filament, a high-energy electron beam is accelerated at a potential of 5-10 kV and it is focused on the substance to be deposited. Because the beam's electrons lose most of their kinetic energy (K.E) as heat, the temperature at the targeted area rises to a high (3000°C), while the rest of the material remains cold. The source material is heated by a filament in the crucible. Electrons are extracted from the filament and focused as a beam on the source material by providing high voltage. To heat the entire material, the beam is swept across the surface of the source material. The substance from the spot point evaporates as it moves towards the substrate, eventually condensing on it. Throughout the deposition process, an ambient chamber pressure is maintained i.e in the order of 10^{-5} torr.

Because the beam of electrons only heats the source material, not the entire crucible, this approach produces a greater density layer with better adherence to the substrate. When compared to heat evaporation, this approach reduces contamination because there is less interaction between the material and the boat. This process also has certain major advantages over other deposition techniques, such as controllable and high deposition rates, as well as high density and better homogeneity of the thin films produced.

2.1.6 Sputtering

2.1.6.1 Sputtering technique

Sputtering is the process of ejecting material from a source material and deposited substance on a substrate held in a vacuum chamber. During the sputtering process, the required deposition pressure is maintained inside the chamber. Materials with high melting points are easily sputtered and thin films are created using the sputter deposition process, however, evaporating the same materials using a resistance evaporator is not feasible. In addition, the composition of the sputtered thin films is identical to that of the source

material, and their adherence to the substrate is better than that of the evaporated thin films. Other benefits of this deposition approach include the use of a sputtering source with no heating parts and the compatibility of the entire setup with reactive gases like oxygen. In most cases, the sputtering gas is an inert gas like argon (Ar). Sputtering begins when a negative charge is applied to the target i.e. source substance, causing a plasma or glow charge. The positively charged gas ions created in the plasma region, ionized A+ ions, are attracted to the negatively biased target material, and collide with it, causing a momentum transfer. [141] These impacts eject atomic-sized particles from the target, allowing them to settle as a thin film on the positive electrode-connected surface of substrate. Secondary electrons are formed when ionized A+ ions collide

with the target surface of the object, aiding the ionization process in the chamber. When the sputtering gas pressure is increased, the chance of ionization rises, and the number of ions and gas conductivity rises as well, lowering the breakthrough voltage. This produces stable plasma, allowing enough ions to be accessible for sputtering the target material during the deposition time. The following are the sputtering procedure parameters that affect the qualities of the produced films:

i.) The sputter current controls the pace at which material is deposited.

ii.) The applied voltage determines the maximum energy with which sputtered particles ejected from the target surface, as well as the sputter yield, or the ratio of sputtered particles to sputtering ions.

iii.) Sputtering gas pressure and distance between target material and substrate – These factors impact the sputtered particles' mean free path and, as a result, the porosity, crystallinity, and roughness of the thin films formed.

iv.) The stoichiometry of the thin films prepared is controlled by the reactive gas mixture.

v.) Substrate temperature – This affects the density of thin films as well as how they grow in terms of crystallinity.

vi.) Bias-voltage to the substrate – This controls the layer's growth by either accelerating or deflecting electrons towards or away from the substrate.

Lower voltage for striking plasma, control of homogeneity, reduction in substrate heating, notably in the case of Si wafers heated by electron bombardment, and high deposition rate are some of the benefits of employing magnetron sputtering. This approach offers several advantages over thermal evaporation, such as the presence of high-energy atoms, a short vacuum path, more collisions, smaller particle sizes, and greater adhesion. This technology is used to produce thin films of various materials in the semiconductor industry for developing integrated circuits. Sputter-deposited anti-reflection thin film coatings on glass substrates have a wide range of optical applications. Contact metals are deposited effectively in thin-film transistor production using this method of deposition because the substrates may be kept at low temperatures. Sensors, photovoltaic cells (solar cells), metal cantilevers, and interconnects are some of the other uses for thin films made this way. Magnetron sputtering has both DC and RF modes, with DC sputtering dealing with conducting materials. Sputtering will be terminated in DC mode in the case of non-conducting materials due to the constant build-up of positive charge on the target material's surface. In RF mode, both conducting and non-conducting objects are sputtered.

W.R. Grove discovered sputtering or sputter deposition in 1852 [142], and it is a conceptually simple approach. When surface of target material i.e. source is bombarded with

high energy particles, the surface atoms can be ejected due to collisions between the surface atoms and the bombarded high-energy particles, a process known as sputtering. When ions bombard the surface of solids, several interactions occur, including ion reflection, secondary ion ejection, ion implantation, and structural rearrangement of the source material caused by ion impact, which results in a number of collisions with target atoms, resulting in atom ejection and revealing the phenomenon of sputtering. The ejected particles can be condensed to form a thin film on a substrate. This phenomenon occurs predominantly in the incident energy range of 100 eV to 1000 keV, with threshold energy of 20 eV. This approach has several advantages over standard evaporation procedures, free from container contamination. It is also feasible to deposit alloy films that retain the target material's composition. radio frequency (RF) sputtering, DC-sputtering , ion beam sputtering, and magnetron-sputtering are the four variants of this technology [143]. In this dissertation, the RF-sputtering technique was utilized to fabricate nanocomposite thin films.

2.1.6.2 Radio-frequency (RF) sputtering

The RF sputtering technology is used to deposit thin layers of insulators and non-conducting materials. Feasible substitution of an insulator for a metal target in dc-sputtering cannot maintain the glow discharge due to the surface charge of positive ions that build up on the front side of the insulator, whereas in RF-sputtering, the dc-power supply is replaced by RF-power supply to keep the glow discharge with an insulator target.

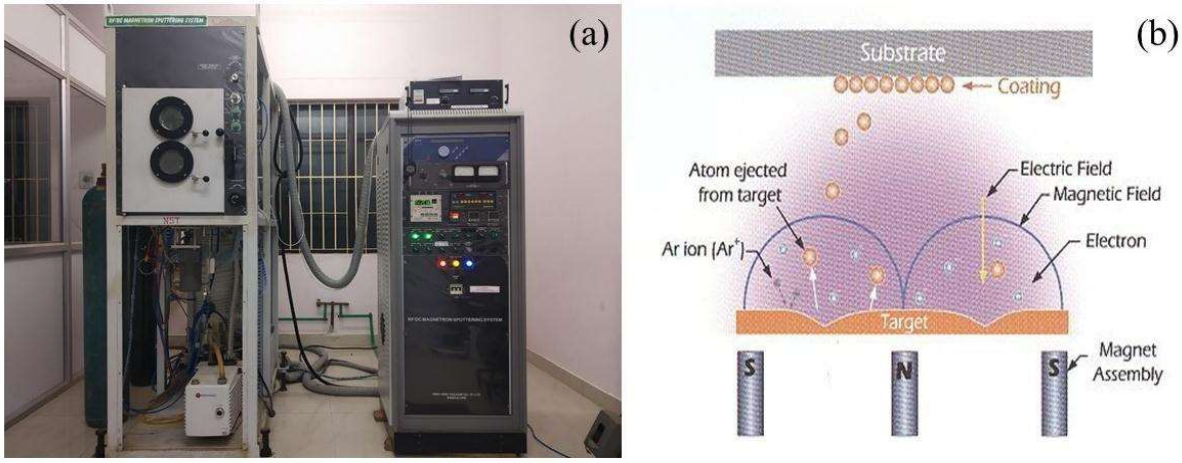

Figure 2.1 (a) Instrumentation picture of reactive RF magnetron sputtering (b) schematicdiagram of ion ejection from target and coating

[140] Impedance matching between the power supply and the discharge chamber is also required for this technique. Because the working pressure was fixed about 10^{-3} Torr, the electrical field during RF sputtering in the chamber enhanced the likelihood of gas molecules colliding with secondary ions. Sputtering is one of the most promising deposition methods, with benefits such as homogeneous deposition on large substrates, improved adhesion, stability, and increased film density.

2.1.6.3 Reactive Sputtering

Sputtering a metal, polymers, alloy materials, or compound in a reactive gas mixture to deposit a compound thin film formed of the sputtered material and the reaction products are known as reactive sputter deposition. This method has produced a wide range of compounds with a wide range of characteristics. Other methods of forming these compounds, particularly at low substrate temperatures, are difficult or impossible in some situations.

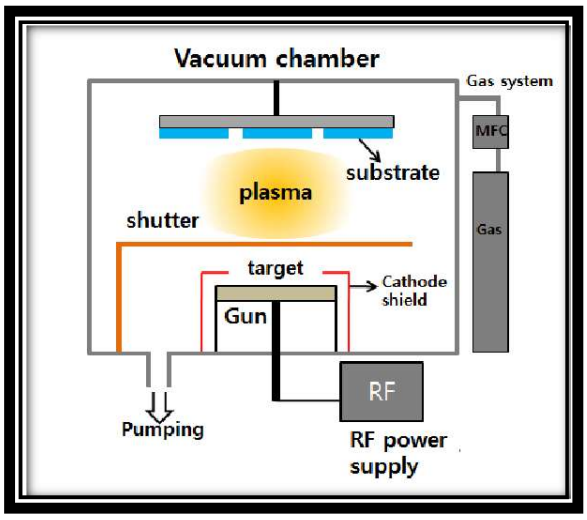

Figure 2.2 Basic setup of RF sputtering method

(http://marriott.tistory.com/97, Retrieved December 2016.)

The sputtering process, discharge of plasma, transport of the sputtered ions and gas ions, the mechanism of film growth, and their chemical interactions at the source and film surfaces all play a role in the reactive sputter deposition process. These elements interact in some way and hence have an impact on the qualities of the films. Reactive sputter-deposited films have a wide range of uses. Deposition of AlN or Al_2O_3 on an Al target and deposition of TiO_2 on a Ti target with the help of N_2 or O_2 gas are examples of reactive sputtering. The layer produced by the sputtering technique would be metallic if a reactive species, such as N_2 or O_2, was not introduced. When a reactive gas species is introduced, it reacts with the sputtered atoms on the target to generate a complex thin film. The films will only be partially activated at low levels of the reactive species. The films will be fully reacted and deviated from the metallic state as the concentration of reactive gas (O_2, N_2, CH_4) in the gas mixture increases. The non-metallic mode of reactive sputter deposition is

when the rate of compound production is faster than the rate of sputtering. This formation of an insulating substance on the target surface reduces the deposition rate because lower sputter yield of the insulating layer compared to pure metal.

2.2 Characterizations Techniques:

The objective of this thesis is to use a reactive RF magnetron sputtering technique to determine nanostructure thin films. XRD, FESEM, UV, Electrical conductivity measurement, FTIR, and Raman techniques can all be used to characterize the thin film nanostructured materials that have been synthesized. As fellows, the basic information about these strategies was presented in brief. X-ray diffraction (XRD) was used to investigate the structural behavior of the fabricated thin-film nanostructure. Field emission scanning electron microscopy (FESEM) was used for morphological and elemental investigation. UV-Visible spectroscopy (UV), Photoluminescence (PL), and Tauc plot were used to investigate the optical behavior of films. The functional properties of the thin film nanomaterials were investigated using Fourier transform spectroscopy (FTIR), and the vibration of the thin film nanomaterials was investigated using Raman spectroscopy (Raman spectra). The surface chemical composition of thin-film nanostructured materials was investigated using X-ray photoelectron spectroscopy (XPS).

Novel material discoveries have played an essential role in the advancement of science and technology. In the development of innovative materials, characterization is a crucial phase. Phase analysis, compositional characterization, structural elucidation, microstructural analysis, and surface characterization are all aspects of material characterization that have a significant impact on material attributes. This has a deficit to the development of a wide range of modern materials science techniques. In this section, Different instrumental

procedures for characterizing thin films that have been produced and processed have been discussed in detail. Scientists working in the field of micro analytical analysis have mostly worked to interpret the structural characteristics of materials down to the atomic level. Other waves, such as X-rays, electrons, or neutrons, must be used to replace visible light (wavelength=4000-8000). Whereas the wavelength of an X-ray depends on the target element, for example, CuK_{α} = 1.5418, the wavelength of electrons can be regulated by the accelerating voltage, for example, wavelength = 0.037 for 100kV electrons. The study of structural and microstructural techniques used for this purpose corresponds to "X-ray diffraction and electron microscopy," which is one of the primary techniques of the current research work. As a result, it will be essential to go through these approaches in significant detail. The descriptions for characterization of as-synthesized (bulk form) as well as transformed materials are included in the following sections.

2.2.1 X-ray Diffractometer

Crystalline solids comprise more than 95% of all solid materials. X-ray diffraction occurs when an electromagnetic wave (the x-ray) collides with a systematic array of scattering sites in a crystalline substance (the atoms are arranged in a repeating pattern within the crystal). As a result, an x-ray diffraction spectrum of a pure substance is similar to a fingerprint. Powder diffraction is an excellent tool for characterizing and identifying polycrystalline phases.

A diffractometer is equipment that is used to examine crystalline and nanocrystalline materials by measuring how they diffract x-rays of a specific wavelength. The x-ray tube and the goniometer are the two important components of an x-ray diffractometer. [144-146] In a cathode ray tube, x-rays are produced by burning a filament to produce electrons, then

adding a voltage to accelerate the electrons towards a target and bombardment the source material with electrons. Characteristic x-ray spectra and bremsstrahlung are formed when electrons have enough energy to displace inner shell electrons of the source material. Cuk$_\alpha$ radiation 0.5418 is the most popular target material for single-crystal diffraction. These X-rays are collimated before being directed at the material. The goniometer uses a large flat substance with a parafocussing arrangement to enhance diffraction intensity, an x-ray detector/counter in place of film to measure diffraction angles, and many electronic circuits to determine diffraction intensity at any angle. The reflected x-rays intensity is recorded as the sample and detectors are rotated. When the circumstances satisfy Bragg's law ($2d \sin \theta = n\lambda$), the incident rays interact with the sample and generate constructive interference. In a crystalline sample, this equation connects the wavelength of electromagnetic radiation to the diffraction angle and lattice spacing. Following that, the diffracted x-rays are detected, processed, and recorded. The counter converts the sample's radiation spectrum into a pulse spectrum, which is supplied into the panel of circuit and analyzed in a variety of ways after appropriate amplification. The pubes, smoothed into a flowing current, may be utilized to actuate a pen on a strip chart and provide a permanent graphic record of intensity vs. diffraction angle, while remaining tangent to the focusing circle along the same axis as the substance but at twice the normal angular speed. Due to the random orientation of the powdered material, scanning the sample across a range of 2θ angles should provide all potential lattice diffraction directions. Figure 2.3 depicts the x-ray optical system of a commercial diffractometer. The focusing error is maintained to a minimum by utilizing a very thin x-ray beam in the plane of the focusing circle (the focusing plane). The line-shaped focus point is seen longitudinally and at an angle of

roughly 30 to the target's surface to produce such a beam. This arrangement's effective source-beam width is less than 1/10 mm. The breadth of a divergence slit determines the beam's actual angular aperture. With decreasing angle of incidence, the length of specimen irradiated by the beam via given slit increases. This establishes a lower limit on the angular range that may be scanned with a given slit-width without surpassing the sample's whole length and risking detection of stray radiation dispersed by the specimen holder. The axial plane of a line-focus beam has a higher divergence than the plane normal to the focusing circle (the axial plane), but this is minimized to a few degrees by the use of a parallel plate assembly. The diffracted beams are controlled in a similar way using a slit and a parallel-plate collimator. The scatter slit near the counter's glass is designed to keep non-diffracted radiation out, lowering the powder spectrum's background. The goniometer radius of this diffractometer is 170 mm, allowing it to fully use the increased resolution provided by the use of a line-focus source, as well as the increased intensity provided by a large specimen.

Diffraction at varying depths in the sample, the divergence of incoming and diffracted beams, and the use of a flat sample are all instrumental factors that impact the position and form of a diffractometer peak. The impact of these elements is often measured using a careful experimental peak. In general, these factors are counted with the use of a highly absorbing sample to limit diffraction to the sample surface and the use of slits and parallel-plate assemblies, as previously described, to reduce beam divergence. A flat sample does not meet the parafocussing condition; only a narrow region can diffract at the proper 2θ angle. The remainder diffracts at a lower angle of incidence, resulting in a broadening of the peak and a shift in the Centre of gravity to a lower 2θ value. Low-angle diffraction has the most significant effects. When the incident beam is held to a 1^0 divergence in the

focusing plane, for example, the flat sample factor has a small impact compared to the effect of cross-divergence, but the constricted beam results in a loss of intensity. As the 2θ angle of the diffractometer is adjusted over its range, Ogilvie [147] describes a mechanism for mechanically curving the sample to fit the curvature of the focusing circle. The precision of wave periodicity is maintained by "coherent scattering." As atoms of various types and positions emit scattered waves, constructive or destructive interference takes place in various directions. The "diffraction pattern," which is composed of constructively interfering waves and the crystal structure of the material has a fundamental geometrical interaction. A material's diffraction pattern is a spectrum of real-space periodicities. Diffraction occurs at small angles for atomic variations with long repetition distances, whereas diffraction occurs at large angles for short repeat distances (as a result of narrow interplanar spacing). It's not difficult to predict why diffraction experiments are important for assessing material crystal structures. The diffraction pattern of material contains a lot more information about it. Diffraction peaks seem to be sharp and clear in crystals with specific patterns over long distances. The atomic arrangements of crystals with defects (such as dislocations, internal stresses, impurities, planar faults, or tiny precipitates) are less precise; however, they still have identifiable diffraction peaks. Their diffraction peaks, on the other hand, are broadened, deformed, and weakened, and "diffraction line shape analysis" is a useful tool for examining crystal defects. And although its diffraction patterns lack strong diffraction peaks, diffraction tests are performed to analyze the structure of

amorphous materials. The incident waves in a diffraction analysis must have wavelengths that are comparable to the distance between atoms.

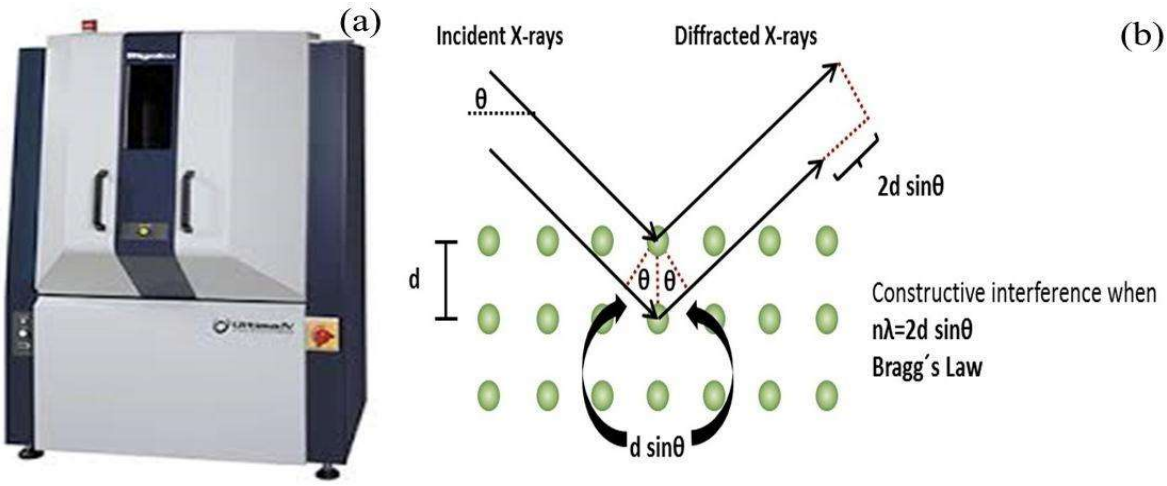

Figure 2.3 (a) Instrumentation picture of X-Ray Diffraction (b) schematic diagram of X-raydiffraction working principle

Determination of crystallite size by Scherrer's formula

The micro residual strain and crystallite size are the main factors of line broadening. the crystallite size (d) is calculated using Scherrer's formula [148, 149] in the case of relatively small miro-residual.

$$D = \frac{0.9\,\lambda}{\beta\,\mathrm{COS}\,\theta}$$

Where the line's broadening (half-width) is at half of its highest intensity, is Bragg's angle, and is the x-ray wavelength employed.

Applications x-ray diffractometers

1.) the most often used approach for identifying unknown crystalline materials is x-ray diffractometry.

2.) It is assessed by observing the structure of crystalline minerals.

3.) Dimensions of the unit cell, such as lattice parameter, bond lengths, and volume, can be determined.

4.) It could be used to determine the purity of the sample.

5.) This approach can be used to determine grain orientation in polycrystalline thin films.

6.) It is utilized to figure out if the deposited thin film and the substrate have the same lattice misfit.

7.) It is possible to estimate the amount of stress and strain obtained in the films. The broadening of the x-ray diffraction peaks can be used to calculate the crystallite size of thin-film samples.

9.) The density of dislocations and the quality of thin films can be estimated. Glancing incidence x-ray reflectivity analyses can be used to assess the density of the films, roughness, and thickness.

Advantages

1.) It is a quick and effective procedure.

2.) In less than 20 minutes, an unknown material can be identified.

3.) In general, it gives unmistakable mineral identification.

4.) There is no requirement for any extra sample preparation.

5.) The interpretation of an x-ray diffraction pattern is rather simple.

6.) This method yields a variety of outcomes, such as morphological characteristics for compositional identification and crystalline lattice information, among others.

7.) It is a non-destructive procedure.

Limitations

1.) For comparing d-spacing, a reference standards file of materials is required.

2.) The detection limit for combined compounds is 2% of the sample.

2.2.2 The Microscopic Technique

When a high-energy electron beam impacts a solid or electron transparent object in an electron microscope, interactions occur. Electrons can backscatter with little or no energy loss from the specimen's front face, or they can interact with surface atoms to form secondary (low energy) electrons. Certain electrons may be absorbed by the substance, resulting in energy transfer to temperatures and, in some cases, lights. Furthermore, Transmitted electrons may remain in the same direction or be scattered at various angles. Electrons can be elastic (no energy loss) or inelastic (energy loss) (having lost some energy). If energy is delivered to the specimen, Auger electrons or X-rays may be produced. Each of these occurrences can reveal details about the atoms in the material. Backscattered and secondary electrons are used to generate surface images in scanning electron microscopes (SEM), while transmitted and scattered electrons are used to form images and diffraction patterns in transmission electron microscopes (TEM). However, the interaction of specimens with high-energy electrons, which produces X-ray, provides information about the atoms within the substances in the region being irradiated, allowing the ultra-structural information in the electron microscope image to be correlated with chemical investigations of very small regions of the substance. Electron probe microanalysis is used to identify X-ray scattering from atoms in a specimen in a scanning electron microscope. In theory, a universal analytical electron microscope (AEM) would be able to see all signals generated within the specimen by high-energy electrons such as

X-rays, Auger electrons, and visible light (cathodoluminescence), as well as electron-hole pairs and induced conductivity effects in semiconducting specimens.

2.2.2.1 Electron Microscopy Scanning (SEM)

The SEM is most commonly used to examine thick (i.e. electron-opaque) samples. Electrons released or backscattered from the substance are collected to give the information:

(1) Information on topography (i.e., the exact geometry of the specimen surface) if secondary electrons having low-energy (less than 50 eV) are obtained.

(2) If greater energy, back scattered electrons are employed, or if leakage current is used, atomic number or orientation information is required. Magnetic domain contrast is revealed by imaging magnetic samples with backscattered electrons. The electron beam-induced current and light cathodoluminescence are two more signals that can be captured.

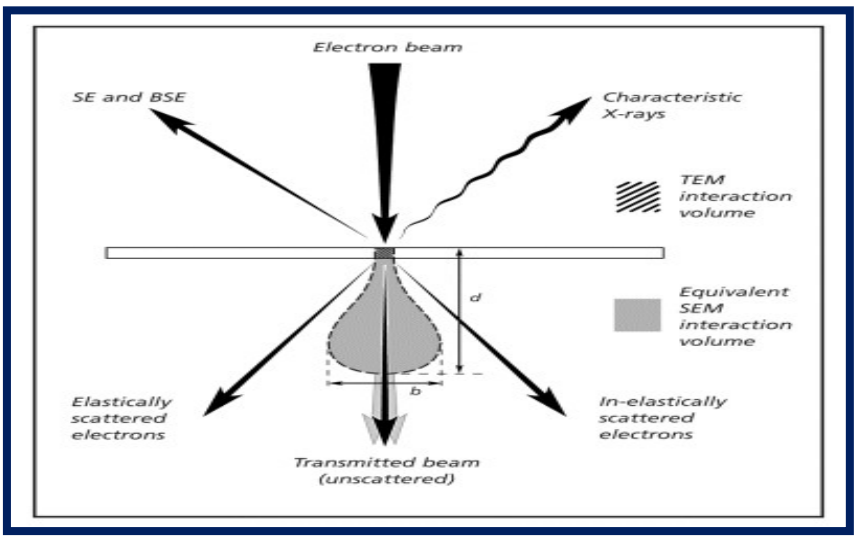

Figure 2.4 Schematic showing main electron interaction with the thin specimen and the information available by analytical microscopy.

The output of the detector can be utilized to regulate the cathode ray tube (CRT) intensity that is scanned at about the same time as the probe on the substance. The ratio of the CRT scan size to the substance scan size determines the image magnification. The image created in this manner is just the variation in signal strength recorded by the detector as a function of the incident probe position.

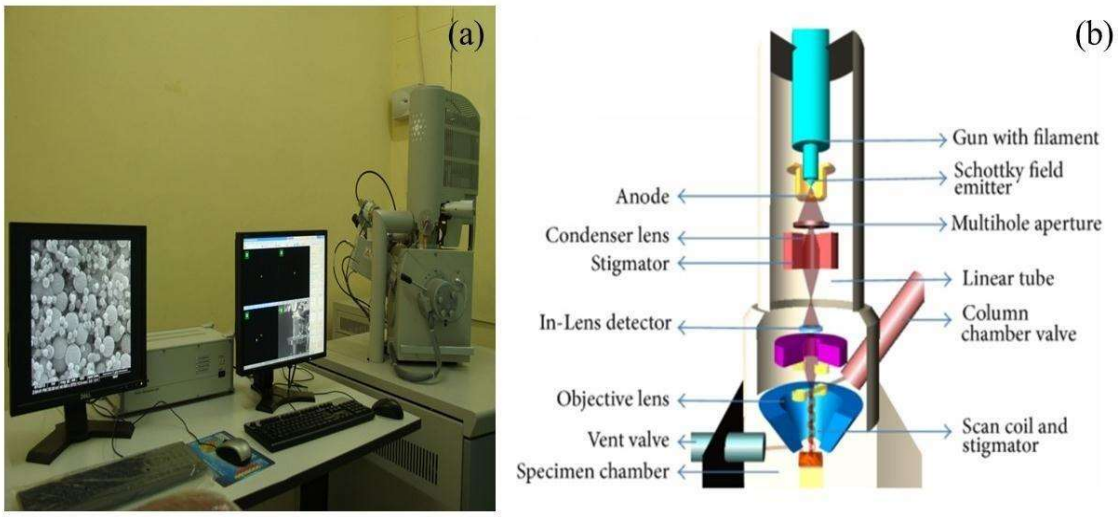

Figure 2.5 (a) Instrumentation picture of Field emission scanning electron microscope (b) Cross-section view of FESEM

Figure 2.5 illustrates a systematic ray diagram for an SEM, with a scintillator-photo multiplier as the most often utilized electron detector. A positive bias of 200 V is supplied to the grid next to the detector if only the highly energetic backscattered charged particles are to be collected, and a negative bias of roughly -200V is applied if only the small energy secondary electrons are to be collected. The secondary electrons will not be affected by this slight change in bias, and backscattered charge particles from the field of view will participate to the image in both circumstances. Solid-state back - scattered detectors are particularly useful in STEM since they may be placed on the bottom probe-

forming lens and are much smaller than scintillator-photo multiplier detectors. The angular dependence of the backscattered electron intensity can be measured by rotating the electron probe over a variety of angles around a fixed point on the material. When these electrons are employed to modify the CRT's intensity, a channeling pattern emerges. Positioning the object in such a way that the charge particles (electrons) strike the surface at a glancing angle produces backscattered electron patterns. Backscattered electron conditions are characterized when electrons are scattered through less than 90 and then Bragg diffracted, causing them to re-emerge from the object. It is observed that no time-dependent input is received because the probe is held constant in this mode of operation, Bragg/ backscattered diffracted electrons are detected utilizing films. As a result, a specific camera must be put inside the specimen chamber for this procedure to work. It is simple to process images in an SEM since the signal is generally generated as a function of time (e.g. to differentiate the signal, to back the signal off, etc.). It is possible to gather X-rays generated by the probe in addition to primary or secondry electrons, and therefore to detect local chemistry. Both energy and wavelength dispersive detectors can be utilized, and the investigation can be done either by positioning the probe on the exact region of interest or by continuing scanning and modulating the intensity of the CRT using X-rays emitted by the element of interest. Unless the scan speed is greatly slowed down, the distribution of specified components can be acquired reasonably quickly by selecting different energy X-rays for subsequent scans. However, these X-ray patterns tend to be quite noisy. In the cathodoluminescent mode, SEM may be utilized to collect information on the distribution of light-emitting regions by modulating the CRT intensity with the light emitted from the sample.

Light-emitting semiconductors can be studied using this imaging modality. In addition, by placing a voltage across the specimen and modulating the CRT with the current in this circuit, the beam-induced conductively can be analyzed. SEM typically operates at 2.5 to 50 kV, with probe diameters ranging from 5nm to 2m at the specimen. The diameter of the probe controls the convergence angle of the probe at the substance. With a depth of field of 2m for a resolution of 10 nm, this is a remarkably large depth of field for such a high-resolution image, highlighting the importance of high magnification SEM images of rough surfaces. The SEM resolution varies depending on the imaging mode, and at least two or three parameters are significant in influencing the resolution-

(1) The maximum allowable magnification is related to the number of lines on the CRT by the expression $M = \delta/d$, where d refers to the specimen size, which is taken here as the probe size, and δ is the screen resolution, which is defined by the number of lines. On a 10cm screen, the number of lines is normally 1000, and the lines are 0.1mm apart (about the resolution of the human eye). If d is likewise measured in millimeters, $M = 0.1/d$ gives the greatest usable magnification, and if M is 1000, the best probe size is 100nm. If the number of lines on the Screen at this resolution is limited to 100nm, a smaller probe size will yield a better image. Most manufacturers have charts that link magnification to probe size, making it simple to select the right probe for the magnification needed.

(2) Since the size of probe affects the resolution of pictures obtained in an SEM analysis, it seems appropriate to utilize a probe with the same order of resolution as the needed resolution. In addition, high angle elastic scattering decreases the resolution considerably, especially at smaller probe sizes.

(3) As stated previously, electron scattering occurs within the sample, the volume of the substance is significant in determining resolution. The degree of resolution deterioration varies with each signal, thus each one will be addressed separately. Light-emitting semiconductors can be studied using this imaging modality.

The incident electrons when they enter the substance, as well as backscattered electrons and X-rays, generate secondary electrons, which give rise to the topological information. The form of the changes in the intensity of the secondary electron signal as depends on distance away from the incident electron probe is shown schematically in Figure 2.5.

The incident electrons generate the central peak in intensity, which has shape of peak that reflects the intensity variance over the incident probe. The incident probe's full width at half-maximum (FWHM) higher is thus a measure of the principal of signal secondary electron. This pattern is superimposed on the much lower backscattered electrons signal generated by electrons that have either been singly elastically scattered or have traveled substantial distances close to the sample surface outside the area identified by the first probe. all backscattered electrons that give rise to secondary electrons are close enough to liberate must suffer at least two high angle elastic scatterings (besides those few energetic electrons scattered near the surface), the intensity of this secondary electron signal produced by high angle elastic scattering electron density will be much lower than that of the signal generated inside the probe’s area. The product of the probabilities of scattering through the two angles reduces the likelihood of an electron being scattered concerning the primary-secondary signal. As the probability of X-ray generation is low, the intensity of secondary electrons produced by X-rays (generated by incident high-energetic electrons) will be low.

According to the description above, high angle elastic scattering can significantly reduce the secondary image in an SEM resolution. As a result, if the background level is modified so that the collected data visible on the CRT values correspond to intensities above the dashed line in figure 2.4, secondary electrons produced by backscattered electrons will not make a significant contribution to the secondary image, and the resolution will be defined largely by the incident probe size. The resolution can be optimised even more by increasing the background level. Signal-to-noise factors define the ultimate limit of resolution because they determine how high the background level can be enhanced. A perfect sample, gold particles on aluminum, would generate a strong secondary signal from the gold and a modest secondary signal from the aluminum substrate due to backscatter, and the sample resolution would be better than size of the initial probe. The drawback must be selected to remove any contribution to the secondary image by backscattered electrons outside the initial probe diameter with more typical samples.

Electrons that experience two or more high angle scattered events and emerge from the substance traveling in a direction where they are captured by the backscattered electron detector alter the spatial resolution of backscattered electron pictures. An experimental value for X-ray resolution and the intensity profile of backscattered images is roughly 2m. Electrons must only be dispersed once through a high angle, after which they may ionize an atom and impair X-ray resolution. Characteristic X-rays have spherical symmetry, and no matter where they are grown in the sample, some will contribute to the signal, even if they are of extremely low energy, in which they will be absorbed. Electrons that have lost a considerable fraction of their initial energy, so cannot be scattered out of the sample can still emit X-rays, the spatial resolution of X-ray signals is expected to be worse than

secondary and backscattered images on this premise as well. Beam-induced and Cathodoluminescence have similar reasoning, and these techniques have typical resolutions of roughly 2 m. Indeed, it is the spatial resolution restriction of SEM that has influenced the creation of STEM in part.

2.2.2.2 Interpretation of Scanning Electron Microscopy Images

The impact of relative insensitivity to crystallographic on electron material interactions and they are as overall similar to optical images, the interpretation of SEM images is relatively significant compared to the interpretation of STEM or TEM images, although it is necessary to consider the important factors that lead to and limit the detailes in SEM images. Individual domains in magnetic samples show contrast, and the source of this contrast will be discussed shortly below. If only secondary electrons (electrons with energies less than 50eV) are collected, the contrast can increase from the following sources: Variation in surface topology (because if the surface is locally nearly parallel with the direction of electron beam, a high secondary electron signal will be produced because many incident electrons will be elastically scattered and travel near the surface of the samples), surface electric fields, surface magnetic fields, and dielectric fields. The topological contrast is the most commonly used of these. When light from the detector, the image of a rough substance seems as if it is viewed from above since the areas of the specimen that have the most direct path to the detector appear brightest. The fact that low-energy electrons are deflected into the detector from places that do not have a straight line of sight into the detector enables for the observation of features within holes and darkened regions-especially if regular image processing is employed to increase contrast within the dark regions. The extraordinarily broad depth of field of SEM in topological models is its

strength. If second phase of charged particles are present in the material, the intensity of the image may be affected by the overall effectiveness of secondary electron generation, which may provide topological interpretation more complicated. Stereo pairs acquired by rotating the substance through the suitable angle can eliminate this issue while also making any height difference much more noticeable. The tilt angle between stereos that are ideal for an individual can changes but is controlled by the height difference and the magnification, just like in TEM. The required tilt angle between the stereo pairs will be short if there are big variations in height (which would require a small divergence angle to produce an appropriate depth of field) and if the magnification is high. For an imaging magnification of 1000 times from a rough surface, a 100 tilt is generally appropriate. In a stereo viewer, the stereo pair should be altered with the tilt axis perpendicular to the line connecting the eyes of the viewer. Most commercial stereo viewers may be used to measure the height difference if the tilt angle and magnification are specified. The tilt angle affects magnification, with the strongest effect in the direction perpendicular to the tilt axis. SEM and STEM impact can be adjusted for in real-time.

The contrast mechanisms that support the non-invasive imaging mode involve atomic number contrast and orientation contrast when backscattered high-energy electrons are utilized to analyze the sample. The backscattered intensity is a component of the incident angle of the electron beam relative to the crystal planes, which generates orientation contrast. The intensity of backscattered light from a crystal for a given direction of electron beam is thus defined by its orientation, and the intensity changes from a polycrystalline substance will cover the range of intensities observable in channeling patterns. This imaging mode, despite its poor contrast, is extremely beneficial for analysing substances

that are difficult to etch or cannot be etched due to the nature of the experiment**.** Again, a minimum beam divergence will optimize the contrast, but it is clear that image intensity drops as the divergence angle decreases, and signal-to-noise concerns can reduce the contrast; the only way to address this problem is to increase brightness and/or scan time. To optimize conditions for each application, the operator must select the optimum balance between magnification, beam divergence, and probe size in SEM imaging. Backscattering efficiency is a function of atomic number, atomic weight contrast develops. Electrons are scattered more efficiently by heavy materials than by light elements. Backscattered images can thus be used to detect compositional changes if the discrepancies result in a change in the terms of atomic weight. The approach is sensitive enough to identify lower differences than one atomic mass unit in mean atomic weight.

Magnetic contrast has been categorized into two types: Type I and Type II magnetic contrast. [150] In Type, I contrast magnetic fields above the surface of specimen influence the low-energy scattered secondary electrons. When the secondary electron signal is used, there is a contrast between domains. This is shown in Type II with secondary backscattered and substance current signals, which are electron trajectories in certain domains that travel near the surface. As a result, the backscattered and secondary electron yields will be increased in these domains, and contrast will be observed.

2.2.2.3 Atomic Force Microscopy (AFM)

Scanning tunneling microscopy (STM) is a type of atomic force microscopy that analyzes the topography of surface electronic states by measuring the tunneling current, which is proportional to the distance between the probe tip and a highly conductive sample surface. We can also analyze with charge density (CDW) using STM. Atomic force microscopy

(AFM), also known as scanning force microscopy (SFM), is a type of scanning probe microscopy that has achieved resolution on the order of fractions of a nanometer, which is more than 1000 times greater than the optical diffraction limit. The scanning tunneling microscope was invented by Gerd Binnig and Heinrich Rohrer at IBM Research - Zurich in the early 1980s and won them the Nobel Prize in Physics in 1985. The first atomic force microscope (AFM) was invented in 1986 by Binnig, Quate, and Gerber [151, 152]. In 1989, the first commercially available atomic force microscope was developed.

The important factors for scanning, materials at the nanoscale can be analyzed with AFM. The data is acquired by using a mechanical probe to scan the surface.

Electric potentials can also be examined by scan through the tip to probe the electrical resistivity or transport of the material surface in some variations, but this is much more complicated, with only a few groups reporting reliable findings. A laser and photodetectors are used to measure the position of the beam in this beam deflection mechanism. The AFM is made up of a cantilever with a sharp tip (probe) which can be used to scan the surface of the material. Silicon or silicon nitride cantilevers with a tip radius of curvature on the order of nanometers are commonly used. Hooke's law states that when the tip comes into contact with a specimen surface, forces between the tip and the substance allow the cantilever to deflect. capillary forces, Mechanical contact force, chemical bonding, electrostatic force, van der Waals force, magnetic force (see magnetic force microscope, MFM), salvation force, Casmir force, and other forces are measured in AFM depending on the situation. In addition to force, other parameters can be monitored at the same time using specific probes (see scanning thermal microscopy, photo thermal micro spectroscopy, etc.). A laser beam reflected from the top surface of the cantilever into an array of photodiodes is often used to

measure deflection. Capacitive sensing, Optical interferometry, and piezoresistive AFM cantilevers are some of the other techniques employed. These cantilevers are composed of piezoresistive components that operate as strain gauges. Strain in the AFM cantilever because of deflection can be detected using a Wheatstone bridge, however, this technique is not as sensitive as interferometry or laser deflection, and there is a possibility that the tip will collide with the surface, causing damage. As a result, most feedback mechanisms are used to modify the distance between tip and sample to keep the force between the sample and the tip constant. The sample is traditionally placed on a piezoelectric tube that may move the sample in the z-direction to maintain a constant force as well as the x and y directions to scan the sample. A 'tripod' design with three piezo crystals; each of these components can be used to scan in the x, y, and z axes. Some of the deformation effects noticed with a tube scanner are eliminated as a result of this. The tip is mounted on a vertical piezo scanner, while the sample is scanned in X and Y using another piezo component. The topography of the specimen is represented by the resulting map of the area s = f(x, y). Depending on the application, the AFM can be used in many different ways. In general, there are two types of imaging modes: static (also known as a contact) and dynamic (or non-contact) modes, in which the cantilever vibrates.

2.2.2.3 (a) AFM Operation Modes

(i) Contact Mode

Contact mode is the most common and extensively used form of functioning. The tip is deflected as it goes over the surface deformations as it is raster-scanned across it. The tip is constantly adjusted in constant force mode to maintain a constant deflection and thus a consistent height above the surface. This modification is what is shown as data. The

feedback circuit, however, limits the ability to follow the surface in this fashion. However, the tip is permitted to scan without this modification, and only the deflection is measured. This is known as variable-deflection mode, and it is useful for high-speed atomic, small resolution scans. Because the tip is in sharp contact with the surface, the lever's stiffness must be smaller than the effective spring constant keeping atoms together, that is on the order of 1 to 10 nN/nm. Figure 2.6 depicts the AFM's contact mode.

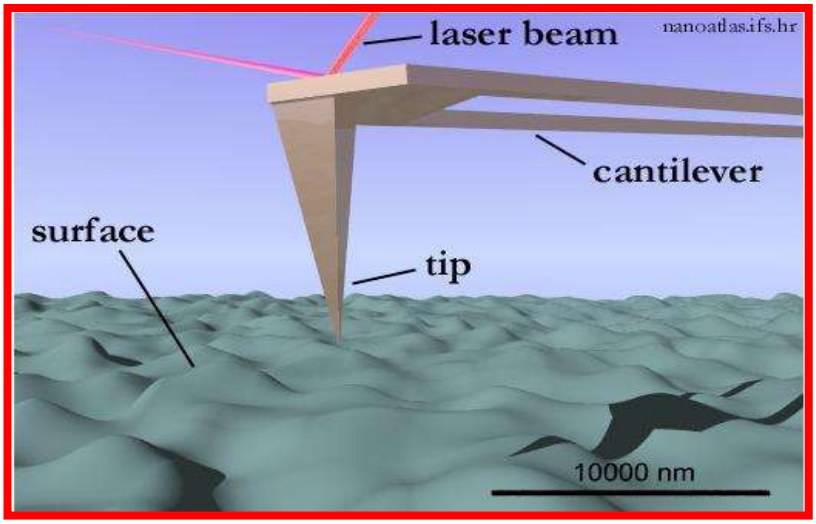

Figure 2.6 The intermittent-contact mode.

(ii) Non-contact Mode

The tip of the cantilever does not make contact with the surface of specimen in this mode. Instead, the cantilever is oscillated at a frequency slightly higher than its resonance frequency, with amplitude of a few nanometers (10 nm). The Vander Waals forces, which are highest between 1 nm and 10 nm above the surface, or any other long-range force that reaches over the surface, serve to reduce the cantilever's resonance frequency. By altering the average tip-to-sample distance, this decrease in resonance frequency paired with the feedback effect system maintains a consistent oscillation amplitude or frequency. The

scanning software can create a topographic image of the sample surface by measuring the tip-to-sample distance at each (x, y) data point. The mode of non-contact AFM does not occur from the tip or sample deterioration effects that can occur with contact AFM after many scans. Non-contact AFM is preferential to contact AFM for soft sample measurement. Contact and non-contact pictures of stiff samples may appear to be the same. If a few monolayers of adsorbed fluid lie on the surface of a stiff sample, however, the images may appear considerably different. In contact mode, an AFM will image the underlying surface by penetrating the liquid layer, whereas, in non-contact mode, an AFM will fluctuate above the adsorbent surface of fluid layer to scan both the liquid and the surface. Frequency modulation and the more prevalent amplitude modulation are two schemes for dynamic mode functioning. Changes in oscillation frequency provide information regarding tip-sample interactions in frequency modulation. Due to the high sensitivity of frequency measurement, the frequency modulation mode allows for the employment of extremely rigid cantilevers. Because stiff cantilevers give stability close to the surface, this approach was the first AFM technique to achieve true atomic resolution in an ultra-high vacuum [153].

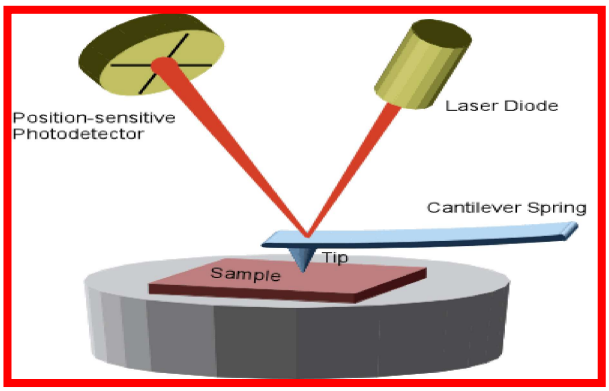

Figure 2.7 Beam deflection systems, using a laser and photodetector to measure the beam position.

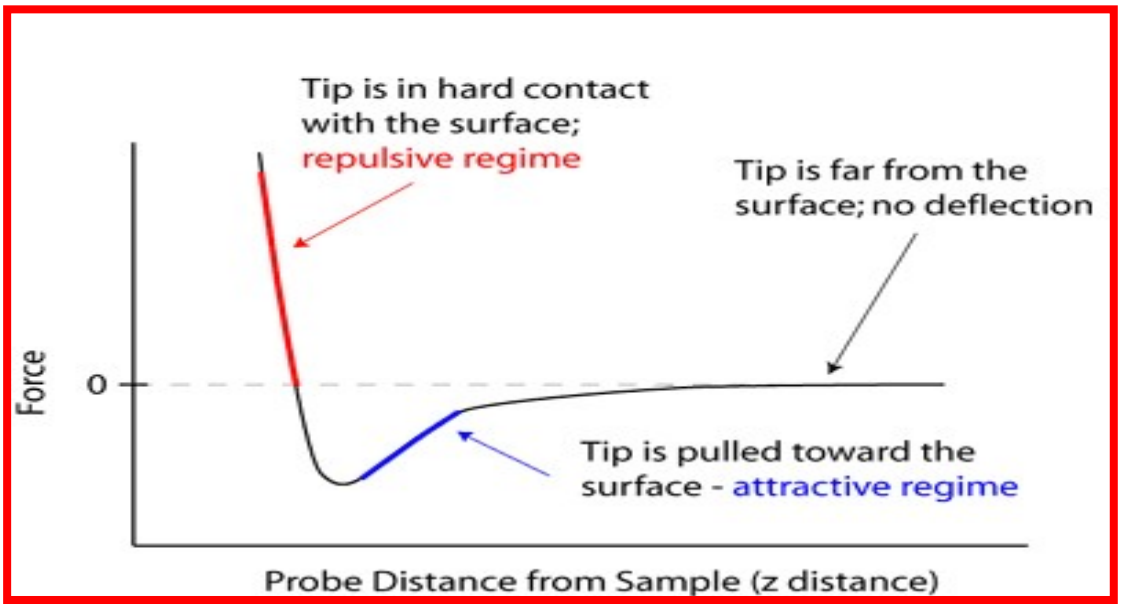

Figure 2.8 The parts of an approach-retraction cycle of the tip.

In amplitude modulation, changes in the amplitude or phase of the oscillation give the feedback signal for imaging. In amplitude modulation, changes in the phase of oscillation can be used to differentiate between various materials on the surface. Amplitude modulation can be performed in two modes: non-contact and intermittent contact. The cantilever oscillates in dynamic contact mode, modulating the separation distance between the cantilever tip and the sample surface. In the non-contact regime, amplitude modulation has been employed with very stiff cantilevers and small amplitudes in an ultra-high vacuum condition to picture with atomic resolution.

(iii)Tapping Mode

Similar to non-contact mode, a smaller piezoelectric device put in the AFM tip holder causes the cantilever to vibrate up and down at approximately its resonance frequency in

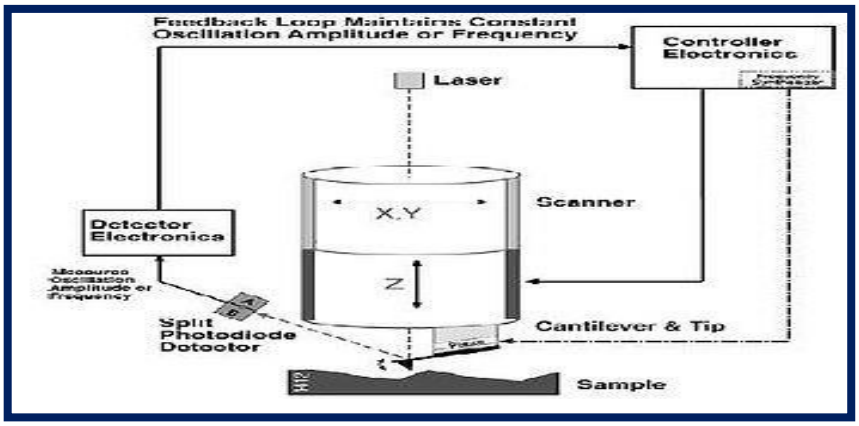

Figure 2.9 AFM - non-contact mode

tapping mode. This oscillation, however, has larger amplitude than 10 nm, usually 100 to 200 nm. The amplitude of this oscillation decreases as the tip gets closer to the substance due to the interplay of forces acting on the cantilever as the tip approaches the surface, such as Van der Waals forces, electrostatic forces, dipole-dipole interaction, and so on.

To adjust the height of the cantilever above the sample, an electronic servo employs a piezoelectric actuator. As the cantilever is scanned over the sample, the servo adjusts the height to keep the oscillation amplitude consistent. The force of the intermittent contacts of the tip with the sample surface is therefore imaged to produce a tapping AFM image. Compared to the amount of damage done in contact mode, this kind of 'tapping' causes less damage to the surface and tip. Even supported lipid bilayers or adsorbed single polymer molecules (for example, 0.4 nm thick synthetic polyelectrolyte chains) under liquid media can be visualized using tapping mode. Single molecules' conformation can be maintained for hours [154] with the right scanning conditions.

(b) Advantages and disadvantages

AFM provides many advantages as Compared to a scanning electron microscope (SEM). The AFM, unlike the electron microscope, which produces a two-dimensional projection or image of a specimen, produces a real three-dimensional surface profile. Furthermore, AFM-viewed materials do not require any additional treatments (such as metal/carbon coatings) that would alter or damage the sample irreversibly. While an electron microscope requires a costly vacuum condition to function properly, most AFM modes may operate in ambient air or even liquid. This allows researchers to examine biological macromolecules and even live creatures. AFM has a better resolution than SEM in theory. In an ultra-high vacuum (UHV) and, more recently, in liquid conditions, it has been shown to give actual atomic resolution. The resolution of a high-resolution AFM is comparable to that of a scanning electron microscope (SEM) or a scanning transmission electron microscope (TEM).

The single scan image size is an AFM disadvantage as compared to the (SEM). The SEM can image an area of square millimeters in one pass, with fields of view of millimeters. The AFM, on the other hand, can only scan objects with a maximum height of 10-20 micrometers and a maximum scanning area of 150x150 micrometers. Using parallel probes in a form similar to millipede data storage is one method of increasing the scanned area size for AFM. An AFM's scanning speed is also a key barrier. Traditionally, an AFM cannot scan images as quickly as an SEM, with a typical scan taking several minutes, whereas an SEM can scan in near real-time, although at a lower quality. The AFM microscope is less appropriate for determining appropriate distances between topographical features on the image because of the comparatively slow scanning rate. [155-157]

However, several fast-acting designs [158-160] have been proposed to improve microscope scanning productivity, including video AFM (With video AFM at video rate: quicker than the average SEM, satisfactory quality pictures may be acquired). Several techniques have been developed to remove visual distortions caused by thermal drift. Hysteresis of the piezoelectric material [161] and cross-talk between the x, y, and z axes can also have an impact on AFM pictures, necessitating software improvement and filtering.

Applications- AFM is mainly used for

i) Analysis of Surface roughness

ii) Thin-film epitaxial deposition step generation

iii) Pin-hole development or other flaws in oxide growth

iv) Assessment of Grain size

v) Material characteristics such as adhesion, elasticity, and surface stiffness, are highly sensitive to changes in phase mode.

2.2.3 Energy Dispersive X-Ray Spectroscopy

For elements with atomic numbers, energy dispersive X-ray spectroscopy (EDX) is a quantitative and qualitative evaluation of the chemical composition of the sample. Scanning electron microscopy and transmission electron microscopy are among the applications it supports. With an electron beam in the range of 10-20 KeV, EDX can give elemental analysis on areas as small as nanometers in diameter. The X-ray is generated in an area where objects are penetrated to a depth of about 2 microns; the specimens emitted are dependent on the substance being investigated, and the image depicts the elemental color mapping. The ionization of an atom occurs when incoming electrons remove an inner shell electron, resulting in X-ray energy.

When an ionization atom returns to its ground state from its excited state, an electron from a higher outer shell occupies the empty shell and releases energy equal to the potential energy difference between the two shells. This energy will be emitted in form of an X-ray or as an auger electron. [162] The detector analysis, which depicts the photon emitted from the samples and can be used for quantitative and qualitative composition analysis, is illustrated in Figure 2.10 (b). In this investigation, we used EDX (Figure. 2.10 (a)) to identify the elemental composition of the material by collecting and analyzing the energy of these X-rays. The energy of X-rays emitted from a material during e-beam bombardment is measured in the EDX spectrum, which generally peaks at the energy levels for which the most X-rays have been received. All of these peaks are specific to a single atom and represent a single element. The more concentrated an element is in a spectrum, the greater the peak in the spectrum. Low-atomic-number elements are difficult to identify using EDX.

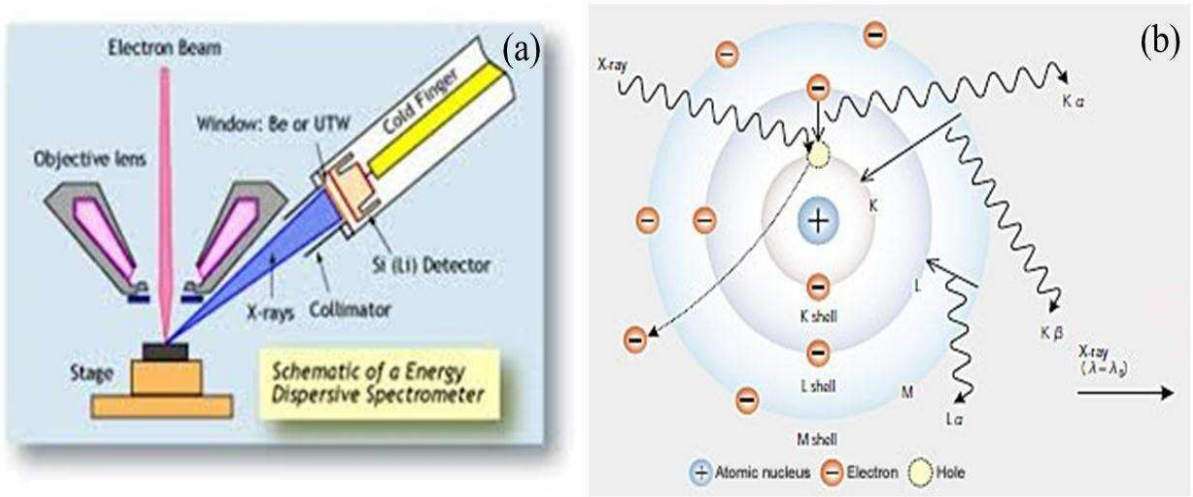

Figure 2.10 (a) Instrumentation picture of Energy Dispersive X-ray spectroscopy (b) schematicdiagram of electron working principle

This analytical device enables non-destructive elemental analysis of the material at the same time.

2.2.4 Electrical Conductivity Measurement

Understanding the electrical characteristics of thin-film can help to determine their applicability for different applications. Electrical properties such as resistivity, conductivity, carrier concentration, and carrier mobility can all be measured using a variety of characterization techniques. In this section, the description and working principle of the four-point probe apparatus are discussed.

2.2.4.1 Four-point probe

Valdes used evenly spaced four-point probes positioned in a line on the surface of thin film to evaluate the sheet resistance (R_{sh}) and resistivity (ρ) of thin films of different shapes and dimensions. [163] The schematic diagram of the longitudinal four-probe configuration is shown in ure 2.11 A constant current is passed through the outside probes, with the help of a source of electricity. The two conducting probes are the potential probes, which are used to determine a floating voltage difference either potentiometrically or with a reliable high impedance digital voltmeter. Valdes established that the resistivity of an infinitely large sample can be calculated using the equation below.

$$\rho = \frac{2\pi V}{I} \Big/ \left(\frac{1}{S_1} + \frac{1}{S_3} - \frac{1}{S_2 + S_3} - \frac{1}{S_1 + S_2}\right)$$

The resistivity is ρ, the floating Voltage difference between both the inner probes is V, the current going through the outer probes is I, and the distance between the probes is S_1, S_2, and S_3. When the probes are evenly spaced, i.e. when S_1, S_2, S_3, S, the equation becomes S_1=S_2= S_3= S.

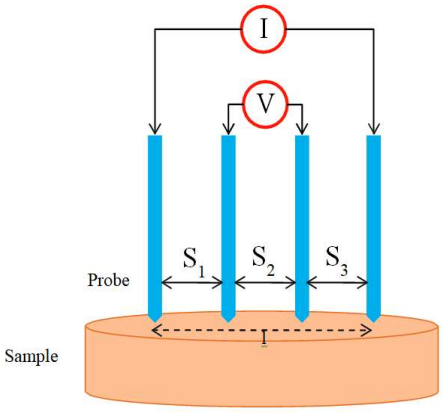

Figure 2.11 Four-point probe technique for sheet resistance measurement

$$\rho = 2\pi S\left(\frac{V}{I}\right)$$

This equation can be applied for samples with a thickness of 0.625 cm or less. The resistivity of samples that are thinner and on a non-conducting substrate is provided by the equation.

$$\rho = \frac{\pi t}{\log 2}\left(\frac{V}{I}\right)$$

Working

The four-point probe method is extensively used to determine a semiconductor layer's electrical resistivity. An electric current flows when an electric field E is applied to a semiconductor material. The electrical conductivity of the layer is calculated by;

$$J = \sigma E$$

The resistance of a rectangular-shaped sample having dimensions l.w.d (where l is the length, w is the breadth, and d is the thickness of this rectangle) is given by:

$$R = \rho\left(\frac{l}{wd}\right)$$

Equations becomes if l = w

$$R = \frac{\rho}{d} = R_s$$

The quantity R_s denotes the sheet resistance of a single square of film, which is independent of the square's size. The four-point probe method is the most popular way of measuring sheet resistance.

$$\left(\frac{\rho}{d}\right) = 4.53\left(\frac{V}{I}\right) = R_s$$

2.2.5 Optical Properties Measurements

2.2.5.1 (a) UV-Vis SPECTROSCOPY (Transmission and Reflection of Light)

A UV-Visible-NIR spectrophotometer capable of measuring in the wavelength range 190-1100 nm is typically used to collect optical transmission and reflection data. A monochromator and a double silicon diode detector have been used in this setup. As an illumination source, a xenon flashlight is employed, with the dual-beam operation mode able to compensate for intensity fluctuations in the source and our surroundings. The resolution and scan speed can be modified or changed to an approximate value. To use the substrate as a reference, a baseline can be recorded. The 45º incidence specular reflectance attachment can be used to record reflection mode data. From the given optical data, values for absorption may be calculated using equations that are given below, and the bandgap value can then be calculated using the arheneous plot. Furthermore, the film thickness can be determined from a fringe pattern for a

known refractive index, or vice versa. As seen in figure 2.12, collimated light incident on a transparent substrate with a thin coating can be reflected or transmitted. The incident light strikes the sample at an arbitrary angle θ_i with regard to the sample surface's normal direction. Part of the light will be reflected at the border at angle θ_r, while the rest will be passed through the sample at angle θ_t.

All three beams, as well as the normal to the surface, must be in the plane of incidence, according to Snell's law (shaded green in figure 2.12). Over a given range of wavelengths, the reflection and transmission observation get the intensity ratios, T and R, respectively. As demonstrated in equations, R and T are defined as the ratio of the light intensity being reflected it or transmitted it over the incoming light intensity I_i on the sample:

$$T = \frac{I_t}{I_i}$$

$$R = \frac{I_r}{I_i}$$

The light from the light source is converged and enters the monochromator, where it is dispersed by the monochromator's grating before converging on the exit slit. The monochromatic light has passed through the exit slit. This light is split into two beams, one for the measurement sample and the other for the reference sample. The light that passes through the sample or the reference sample alternatively strikes the silicon photodiode.

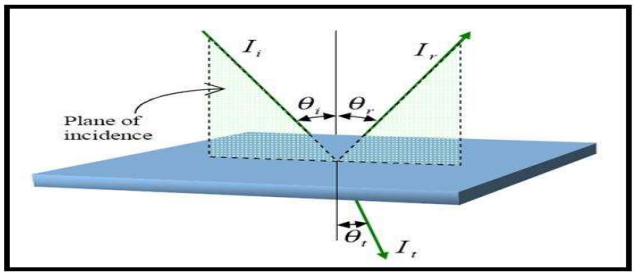

Figure 2.12 Schematic diagram of the incident, reflected, and transmitted beams.

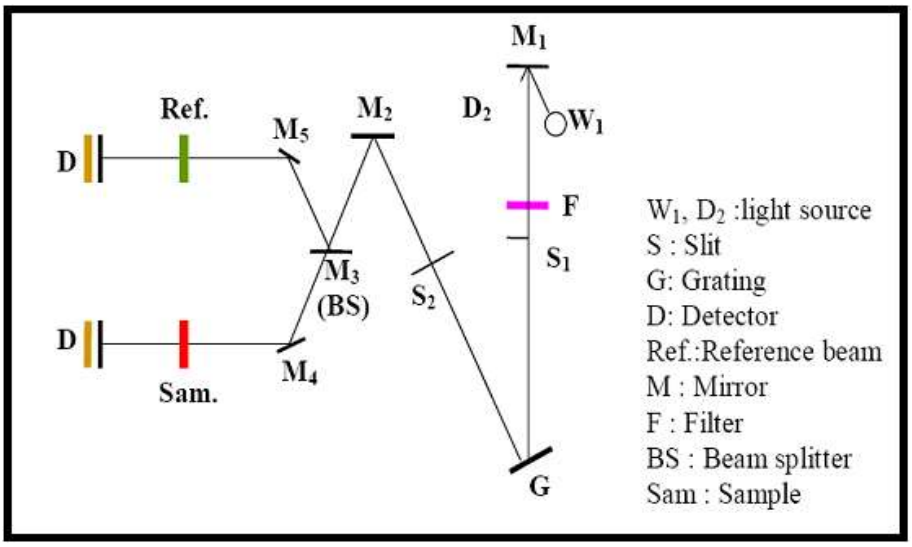

Figure 2.13 Schematic Diagram of Double Beam UV-Vis Spectrophotometer.

2.2.5.2 Fourier transform infrared Spectroscopy

The chemical binding arrangement of the thin film was investigated using Fourier transform infrared spectroscopy (FTIR) in the range of wavenumber 4000-400 cm^{-1}. When infrared radiation is passed through a sample in infrared spectroscopy, some of it is absorbed by the substance and some of it is transmitted. The resultant spectrum depicts the sample's molecule transmission and absorption, resulting in a molecular fingerprint. The spectral analysis of two different molecular structures will not be the same. Figure 2.15 (b) shows the schematic diagram of the FTIR utilized to investigate the deposited films, the interferometer produced the infrared radiation signal at all wavelengths. By using a beam splitter, the incoming infrared beam was separated into two optical beams. One beam reflects off of a fixed flat mirror, while the other reflects off of a moving flat mirror that is only a few millimeters away from the beam splitter. When the two reflected beams from mirrors meet again at the beam splitter, they are recombined. The signal that exits the

interferometer is the consequence of these two beams interfering with each other because one beam's path is fixed and the other's is

continually changing as its mirror moves. The resulting signal is known as an interferogram, and it has the unique property of including information on each infrared frequency that comes from the source in every data point (a function of the moving mirror position) that makes up the signal. This means that all frequencies are measured simultaneously while the interferogram is measured. The observed interferogram signal cannot be analyzed directly since the analyzer requires a frequency spectrum (a plot of the strength at each particular frequency) to make an identification. It is necessary to have a method of decoding the specific frequency. The Fourier transformation, a well-known mathematical technique, can be used to observe this. The computer does this change and then offers the user the necessary spectral data for analysis. [164]

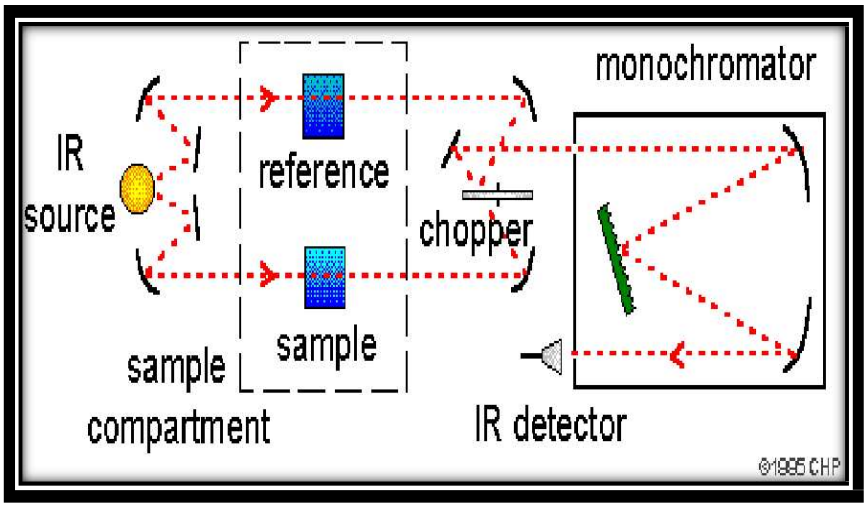

Figure 2.14 Schematic diagram of FTIR.

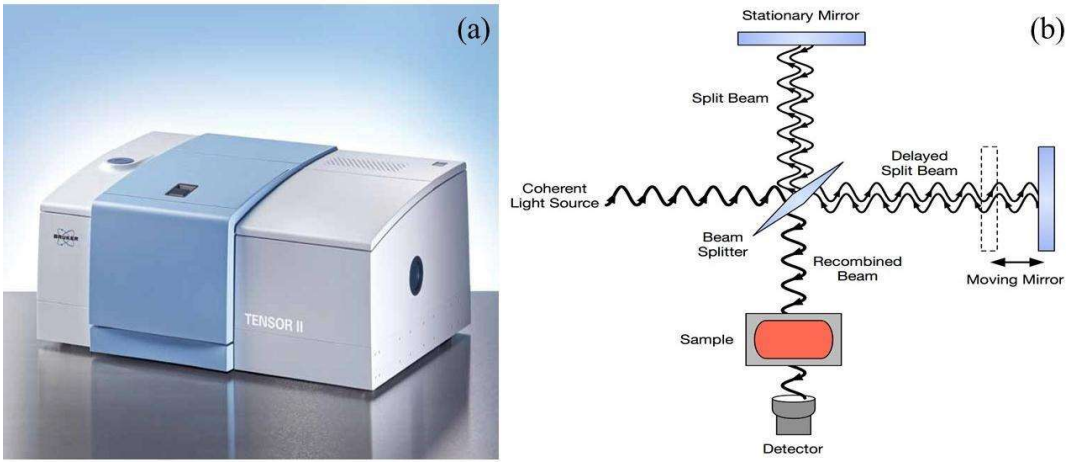

Figure 2.15 (a) Instrumentation picture of Fourier transform infrared spectroscopy (b) schematicdiagram of FTIR working principle

2.2.5.3 Raman spectroscopy

Raman spectroscopy is a vibrational spectroscopic approach for identifying organic and inorganic species, as well as determining the crystalline nature of solids. It uses inelastic light scattering by matter to probe the structure of gases, liquids, solids, and amorphous and crystalline materials. It is not affected by charging effects, which can influence electron and ion beam approaches. [165] The Raman Effect, initially observed by Raman in 1928 [166], is the basis for Raman spectroscopy. If a portion of the incident photon's energy is transferred to the lattice in the form of a phonon (phonon emission), the incident photon becomes a lower energy photon. Stokes-shifted scattering is known as the down-converted frequency shift. Anti-stokes shifted scattering occurs when a photon absorbs a phonon and emerges with a greater energy. The anti-stokes mode is substantially weaker than the Stokes mode, and it is frequently Stokes-mode scattering that is measured. A laser beam, referred to as the pump, is impinging on the sample during Raman spectroscopic observations. To reject Raleigh scattered light, the weak scattered light or signal is transferred via a double

monochromatic; the Raman shifted wavelengths are described by a photo detector. A laser lights the sample through with a commercial microscope in the Raman microprobe. To avoid sample heating and specimen degradation, laser power is typically kept below 5mW. It is required for the pump to be a bright, monochromatic source to differentiate the signal from the pump. The weak signals against the high background of scattering pump radiation consider detection difficult. When Raman radiation is seen at right angles to the pump beam, the signal-to-noise ratio improves. The interference induced by fluorescence, either of contaminants or of the sample itself, is a significant constraint in Raman spectroscopy. Combining Raman spectroscopy with Fourier Transform Infrared Spectroscopy eliminates the fluorescence background problem (FTIR). The Raman spectrometer is extremely sensitive to crystal structure. Various crystal orientations, for example, produce somewhat varied Raman shifts. Because of the stress and strain in the thin layer, the frequencies are also altered. When a beam of monochromatic light strikes on a sample, It is absorbed by the substance and scattered in this method. An objective lens with holographically governed gratings collects the inelastically scattered light. Monochromators' dispersed light is frequently observed using cooled charge-coupled device (CCD) detectors, and the results are shown as a Raman spectrum. The intensity of in-elastically scattered light is depicted as a function of the radiation's wavenumber shift. Each peak in the spectrum corresponds to one or more vibrational modes of solid. When laser light interacts with photons or other excitations in the system, the energy of the laser photons is moved up or down in Raman spectroscopy. The vibrational, rotational, and other low-frequency transitions inherent in the molecules are revealed by the energy shift. Raman measurements do not require sample preparation and can be collected under ambient environments, resulting in high-quality

Raman spectra in less than 2 seconds. As a result, the Raman spectrum shows that carbon has a very basic structure, with three main vibrational bands labeled G, D, and 2D. Even while only three main vibrational bands dominate the carbon spectra, they provide crucial information regarding carbon and coating thickness, which may be determined by assessing the band peak position, shape, and intensity. With laser excitation lines of 514 and 632 nm, Raman spectra were obtained using a Raman spectrometer (Fig. 2.16 (a & b)). [167]

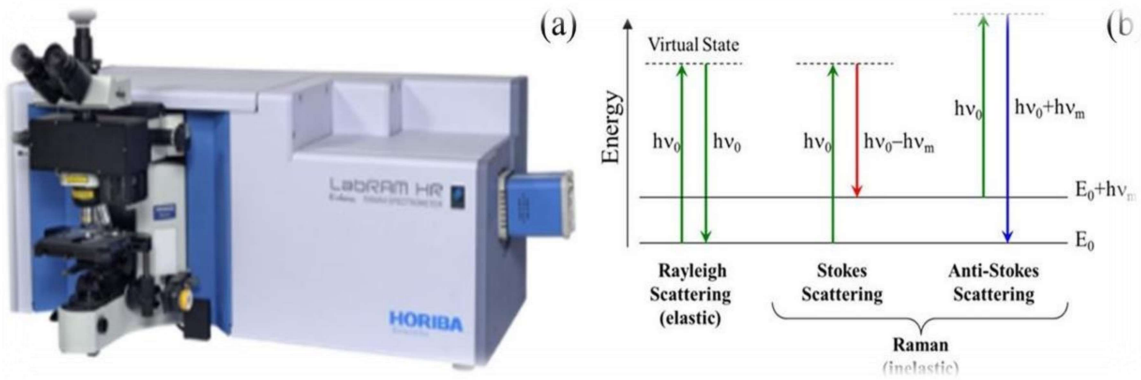

Figure 2.16 (a) Instrumentation picture of Raman spectroscopy (b) schematic diagram of Raman working principle

2.2.5.4 Optical band gap determination

The absorption of incident photons by the material is an important approach for determining the bandgap of a semiconductor. Photons of a specific wavelength are focused on the substance, and the relative transmission of the different photons is measured. The experiment provides an accurate measure of bandgap because photons having energies greater than the bandgap energy are absorbed while photons with energies less than the bandgap energy that is transmitted. [168] For the parabolic band structure, the relationship between the absorption coefficient (α) and the bandgap of the

is given by, according to Bardeen et al.[169]

$$\alpha = \frac{A}{h\nu}(h\nu - Eg)^{r}$$

Where r =1/2 denotes allowed direct transitions, r =3/2 denotes forbidden direct transitions, r =2 denotes allowed indirect transitions, and r =3 denotes forbidden indirect transitions. A is the parameter that is affected by the probability of a transition. Using the relationship, the absorption coefficient can be calculated from the transmission or absorption spectra.

$$I = I_0\ e^{-\alpha t}$$

Where I represent the transmitted intensity of light, I_0 represents the incident intensity of light, and t is the film's thickness. $(\alpha h\nu)^2$ will have a linear dependence on the photon energy $(\alpha h\nu)^2$ in the event of a direct transition. A straight line will be drawn when plotting $(\alpha h\nu)^2$ versus hν, and the intercept on the energy axis at $(\alpha h\nu)^2$ equal to zero will yield the bandgap.

The equation on allowed transition-

$$\alpha = \frac{A}{h\nu}(h\nu - Eg)^{1/2}$$

Squaring at both sides,

$$\alpha^2 = \frac{A^2}{(h\nu)^2}(h\nu - Eg)^1$$

$$(\alpha h\nu)^2 = A^2(h\nu - Eg)$$

For straight behavior, direct bandgap

$(\alpha h\nu)^2 = 0$, then

$$A^2(h\nu - Eg) = 0$$

$$A^2 \neq 0, \qquad h\nu = Eg$$

As a result, the bandgap is directly determined by the x-intercept of the plot produced between $(\alpha h\nu)^2$ and $h\nu$.

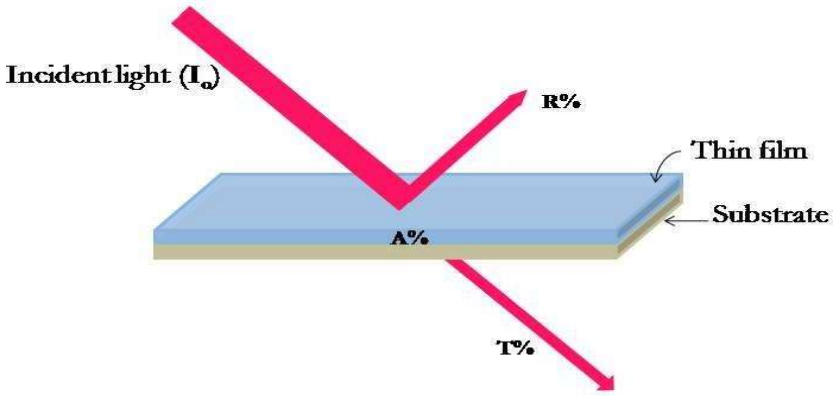

Figure 2.17. Partial reflection, absorption, and transmission of light in a thin film

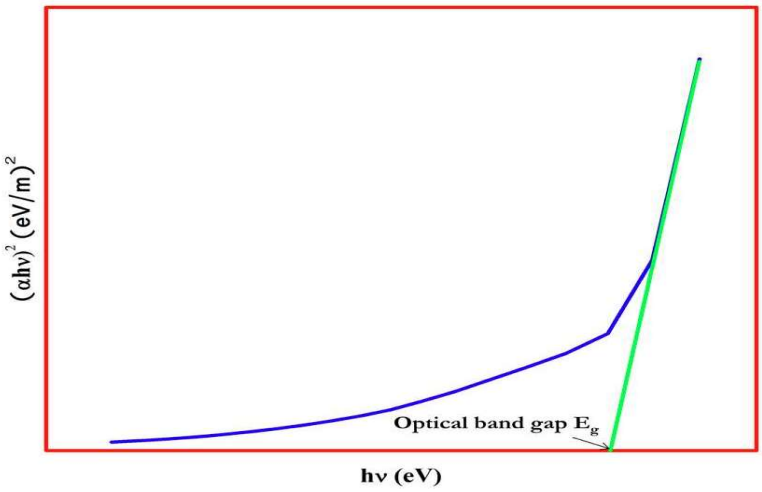

Figure 2.18. Variation of $(\alpha h\nu)^2$ as a function of $h\nu$

2.2.5 Theoretical Calculation

Koelling and Arbman [170] developed the first implementation in 1975, but only with the Muffin Tin (MT) approximation and without advancing to self-consistency. It was extended to a full band structure code in the following years, mostly by Freeman and coworkers [171, 172] who produced the required algorithms and computer codes. Several groups modified this approach and created their programs in the 1980s. One group of them developed the WIEN code [173] over the last 20 years and is currently used by over 500 groups around the world. A book by Singh [174] contains a good analysis of sources related to the LAPW approach. The LAPW basis set made it computationally feasible to go beyond the muffin-tin approximation and address a crystal potential (and charge density) of any shape, effectively turning LAPW into a full-potential scheme. This is especially essential for more complicated materials with open structures or for surfaces that can be addressed by supercells with different periodic boundary conditions.[175] The forces that act on the atoms were another essential variable of interest. The analysis of forces was performed in the WIEN97 code [176] based on the framework of Yu et al. [177], allowing for efficient optimization of structural parameters. For the calculation of structure factors that can be compared with X-ray diffraction experiments, the general shape of the electron density (beyond MT) is important. [178] The electric field gradient (EFG) tensor is a variable related to the ground state density that is sensitive to the anisotropy of the charge density close to the nucleus and can be measured via nuclear quadrupole interactions. [173] The core, semi-core, and valence states are the three categories of electronic states. The core states are totally contained within the atomic sphere and are regarded as thawing cores on an atomic level (fully relativistically), with the relevant density computed in each

iteration cycle using the MT component of the actual crystal potential. The valence states are (partially) delocalized, and the valence density is obtained using the LAPW method. However, Semi-core states are high-lying core states with a fundamental quantum number one lower than valence states. [179] Because they are not completely enclosed within the atomic sphere, they require special attention.